Supporting Information

Efficiency

A new cell setup was procured with an improved layout for gas detection and determination of faradaic efficiency.

Fig. S1: New cell setup in metal cell with separated counter electrode compartment, direct access to headspace and improved sealing. Area of the film is determined to be 6.79 cm^2

Calibration of the gas chromatograph with % H_2 (in Ar) to detector response (in μV) was conducted and presented in Fig. S2. The molar evolution of H_2 per second is determined using the known flow rate of Ar (2 mL min^{-1}), the calculated % H_2 and the molar volume of gas (24.5 L mol^{-1}).
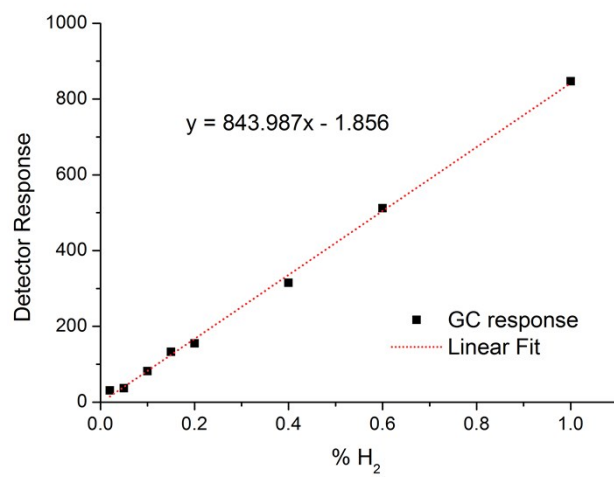
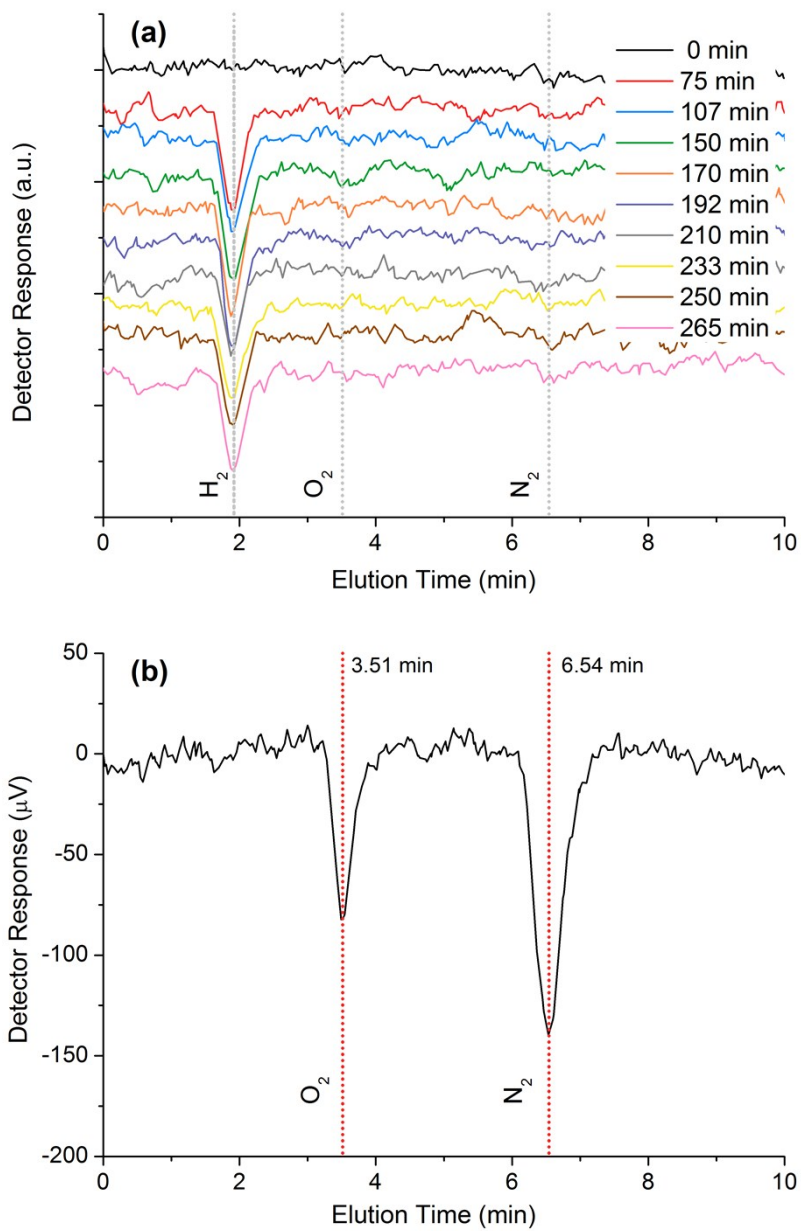**Fig. S2:** Calibration curve relating GC detector response and % H_2

Fig. S3: (a) GC of injected headspace showing detected H_2 for the determination of faradaic efficiency, Ar flow = 2 mL min^{-1}. **(b)** GC injection of air showing its characteristic O_2 and N_2 peak at 3.51 min and 6.54 min respectively, Ar flow = 0.15 mL min^{-1}.

Stability Testing

Full stability CA

Correction of Light Intensity

The correction for the lamp intensity was done utilising an Edmund Optics LaserCheck power meter (model 54-018) with a silicon cell; the power measurement was conducted at a wavelength of 488 nm. An initial power reading (in mW) was taken at 3.9 days and used as the baseline power (100% lamp intensity). Subsequent readings were converted to a percentage based on this initial reading and compared with the photocurrent. Once the decrease in light output is accounted for, the decrease in photocurrent from day 4 to day 12 is *ca*. 80%; as compared to *ca*. 60% without the correction.
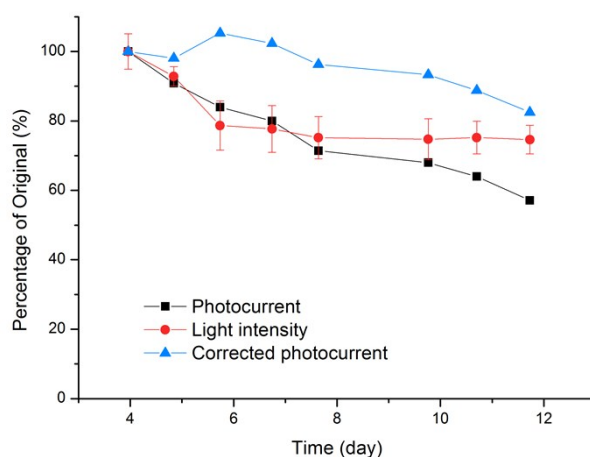

Fig. S4 Longterm percentage decrease from day 4 to 12. The ─▲─ trace shows the corrected decrease in photocurrent when the decrease in light intensity is accounted for.

Counter Electrodes

Initial tests utilising a stainless steel and platinum wire as counter electrodes resulted in a dramatic decrease in photocurrent over time. The comparison between these counter electrodes is shown in Fig. S5 where Ti mesh (black trace) is shown to retain the best long term performance.
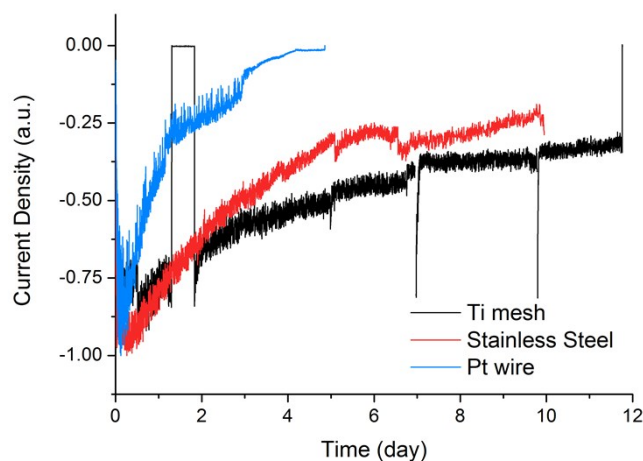

Fig. S5 Comparison of the CA trace of each counter electrode material, all were conducted on the standard PBTh film at -0.5 V vs Ag/AgCl in 1 mol L^{-1} phosphate buffer. They have been normalised to their maximum reduction current for better comparison of their degradation over time.

Subsequent studies using SEM and EDX shows the presence of deposited precipitates of various metal ions, refer to Fig. S6 and Fig. S7 respectively. Different counter electrode materials exhibited slightly behaviour with stainless steel showing substantially higher depositions of metal. This is unsurprising due to the relative reactiveness of stainless steel which would oxidise at higher rates than that of Pt or the mixed metal oxide layer on the Ti mesh electrode. Nonetheless, despite a higher resistance to oxidation, all samples exhibit noticeable metal deposits.
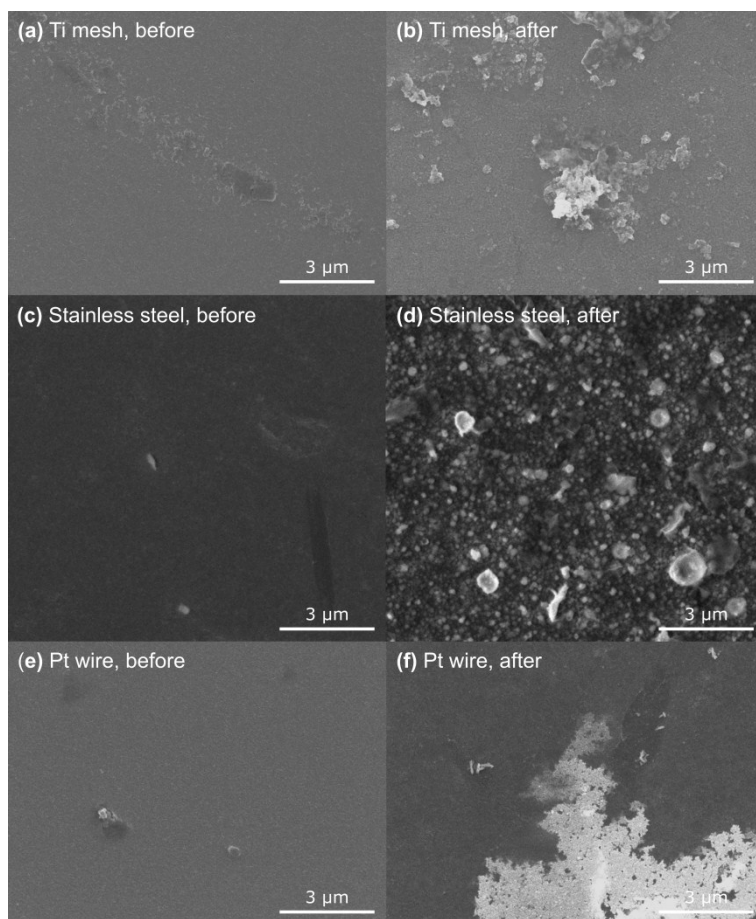
Fig. S6 SEM showing the PBTh film, before and after lonterm stability testing with different counter electrodes. The deposition of precipitates are observed throughout all samples.
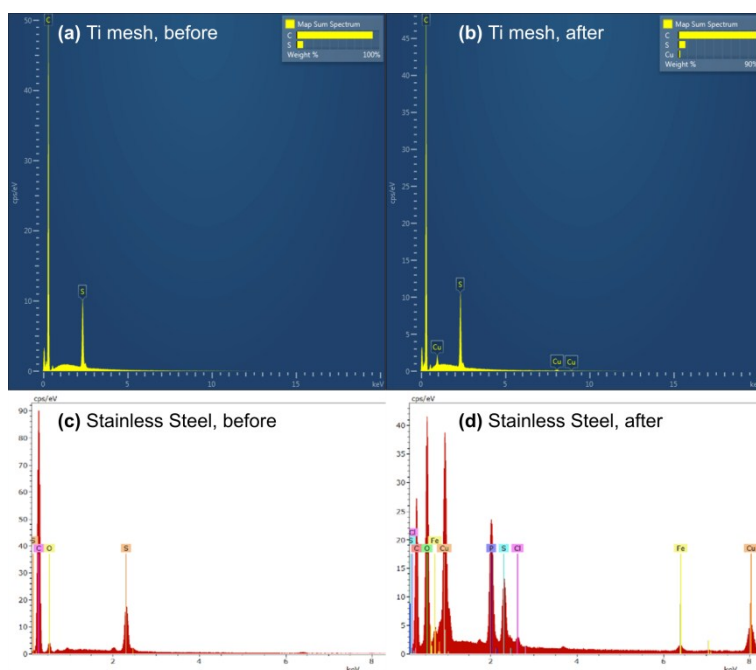

Fig. S7 EDX showing the significant presence of metals after stability testing, prior to testing, all films only exhibited the expected C and S peaks associated with PBTh. The stainless steel electrode resulted in a significantly higher amount of deposition and is reflected in the EDX spectra (d). Pt wire showed an EDX spectra similar to that of Ti mesh.

Calculation of turn over number (TON)

To calculate the total amount of hydrogen produced (assuming faradaic efficiency is 100%) integration of the current density (A/cm^2) over time (s) over the 12 day period was done to determine the total amount of charge. This resulted in a value of 60.1 C/cm^2. Converting to an amount of H$_2$ gas:

$$No. \ of \ e^- = 60.1 \times 6.241 \times 10^{18} = 3.75 \times 10^{20} \ e^-/cm^2$$

$$No. \ of \ H_2 = 3.75 \times 10^{20} \div 2 = 1.88 \times 10^{20} \ H_2/cm^2$$

To determine the number of catalytic sites, given the hydrophobicity of PBTh, we assume that only the first 5 nm of the material is permeable to H$_2$O and catalytically active. Thus:

$$Volume \ PBTh \ reacting = 1 \ cm^2 \times 5 \times 10^{-7} cm = 5 \times 10^{-7} cm^3$$

Density of PBTh = 1.52 g/cm^3

$$m(PBTh \ reacting) = 1.52 \ g/cm^3 \times 5 \times 10^{-7} cm^3 = 7.6 \times 10^{-7} g$$

Assuming one catalytic site is one unit of polymerised bithiophene, M$_r$(catalytic site) = 164.2 g/mol

$$mol(catalytic \ sites) = 7.6 \times 10^{-7} g \div 164.2 g/mol = 4.63 \times 10^{-9} mol$$

$$No. \ of \ catalytic \ sites = 4.63 \times 10^{-9} \times 6.022 \times 10^{23} = 2.79 \times 10^{15} sites$$

$$\therefore TON = \frac{1.88 \times 10^{20}}{2.38 \times 10^{15}} = 6.7 \times 10^4 \ per \ cm^2 of \ PBTh$$
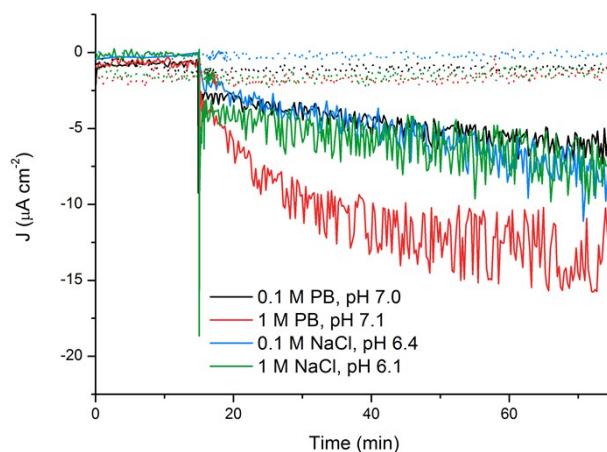
Electrolyte

Fig. S8 CA trace at a potential of -0.5 V vs Ag/AgCl in different electrolytes under bubbled N$_2$. Solid traces represent PBTh films, dotted traces represent glassy carbon under the same conditions. Light was switched on at 15 min, current was recorded at 75 min (after 60 min of illumination).

pH

The pH of the electrolyte was recorded before and after each CV test to ensure that pH had been maintained; this is presented in Table S1.

pH Test	pH before	pH after
3	3.1	3.2
5	5.0	5.2
7	7.0	6.9
9	8.5	8.9
11	11.0	10.9

Fig. S9 shows the CV traces in light, dark and the corrected trace showing the determined onset potential and E^0 at various pH.
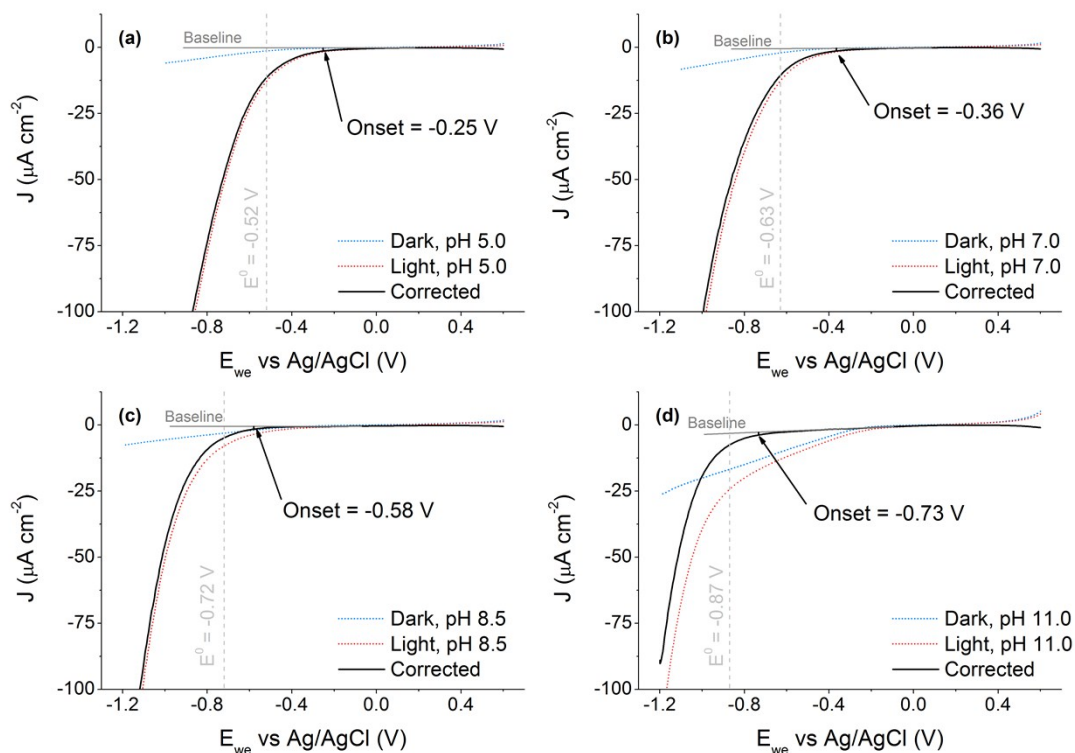

Fig. S9 CV of the PBTh film at different pH showing the determined onset potential, E^0 at the specified pH, the original dark and light traces and the corrected trace. (a) pH 5.0, (b) pH 7.0, (c) pH 8.5, (d) pH 11.0. pH 3.1 is shown in the main manuscript.
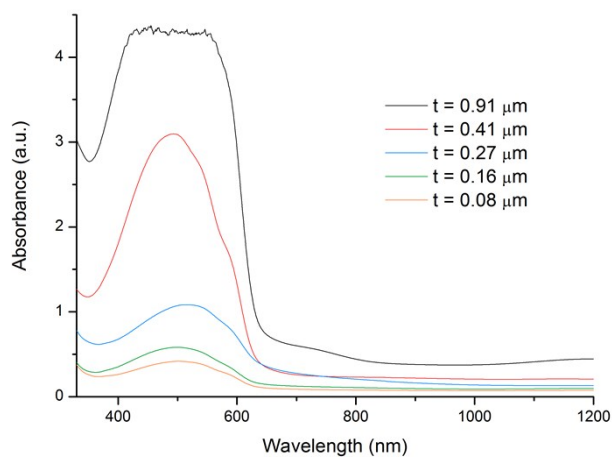
Thickness

Fig. S10 UV-Vis absorption spectra of various PBTh film thicknesses on glass slide. The absorbance of the 0.91 μm film resulted in saturation of the detector and is not presented in the main manuscript, Fig. 6
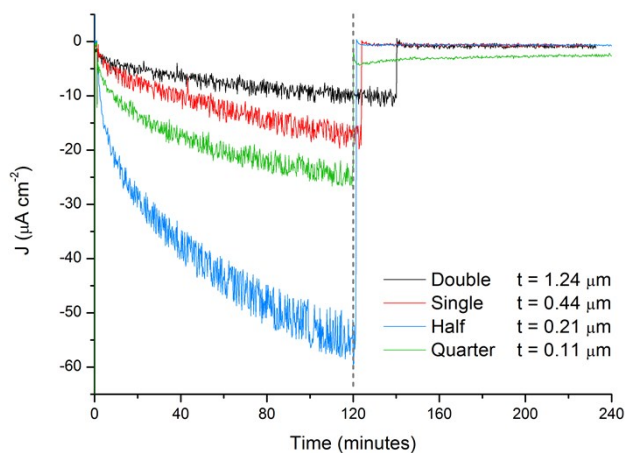

Fig. S11 CA measurement of different thickness with an applied potential of -0.5 V vs Ag/AgCl. The current is recorded at 120 min for comparison (dotted grey line) in Fig. 6. The measured thickness of each film is also shown in the legend.
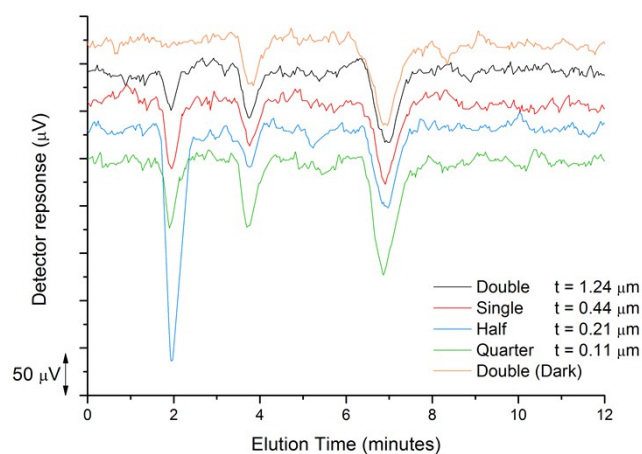
Fig. S12 Gas chromatograms of the injected headspace at 120 min and the recorded H_2 peak at 2 min. Ar bubbling rate was 0.15 mL min^{-1}; O_2 and N_2 can also be observed. The measured thickness of each film is also shown in the legend.
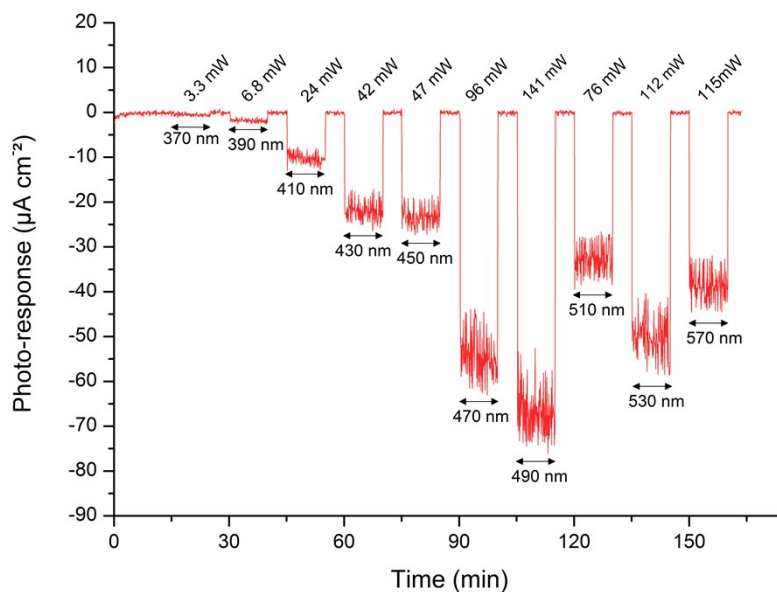
Wavelength dependency

Fig. S13 CA measurement at -0.8 V vs Ag/AgCl in 1 mol L^{-1} phosphate buffer (pH 7) for wavelength dependence measurements; E_0(HER) = -0.63 V vs Ag/AgCl. The photo response is the average current over the 10 min interval with light. The wavelength and corresponding intensity of each band pass filter is also provided.